Nonequilibrium Contributions to the $^{51}V(p, n)^{51}Cr$ Reaction for $18 \leq E_p \leq 26$ MeV*

S. M. Grimes, J. D. Anderson, J. C. Davis, and C. Wong
Lawrence Livermore Laboratory, Livermore, California 94550
(Received 16 July 1973)

Neutron spectra from the $^{51}V(p, n)^{51}Cr$ reaction have been measured at bombarding energies of 18, 20, 22, 24, and 26 MeV. The portion of the spectra corresponding to residual excitations of 10 MeV or less was compared to a shape calculated under the assumption that the residual levels are two exciton proton-particle neutron-hole states. Good agreement was obtained at 22, 24, and 26 MeV, but the spectra at lower bombarding energy could only be fitted with the addition of contributions from four exciton states. The inclusion of pairing effects improved the agreement between the calculation and the data. The data were also compared to a calculation with the hybrid model for preequilibrium reactions; good agreement was observed.

[NUCLEAR REACTIONS $^{51}V(p,n)^{51}Cr$, $E_p = 18, 20, 22, 24, 26$ MeV; measured $\sigma(E_n, \theta)$, $\theta = 24$–$144°$.]

I. INTRODUCTION

Two recent papers[1,2] have compared the nonequilibrium portions of (p, n) spectra for neighboring targets in order to test the prediction[3] that different shapes should be observed for even-A and odd-A targets. These comparisons are essentially tests of the assumption[3] that the odd nucleon in an odd-A nucleus is likely to be rescattered in the first (or first few) stages of a nonequilibrium (p, n) reaction.

The exciton[3-6] model for preequilibrium reactions rests on the assumption that the compound nucleus reaches an equilibrium state through a series of two-body interactions. The initial single-particle state decays into a two-particle–one-hole state, which in turn decays to a three-particle–two-hole state. It is assumed that at each stage the particle-hole states can decay through emission of a particle as well as by damping into a more complex state. These decays result in a preequilibrium contribution to emission spectra.

Quantitative results can be obtained only by assuming specific forms for the densities of levels of specific particle-hole configuration. A closed form results if it is postulated that the single-particle states are equidistant in energy and that densities for multiple particle and hole states can be obtained by folding together the single-particle density the appropriate number of times. In such a case it may be shown that the density of n-exciton states (where n is the sum of the particle and hole number) is proportional to U^{n-1}, where U is the excitation energy. For a (p, n) reaction, the residual states reached by decay from a two-particle–one-hole state will be of one-particle–one-hole type and would therefore have a level density varying as U. If it is assumed in addition that the odd nucleon is scattered in the first stage of the reaction, the residual states would be two-particle–one-hole states, which for the constant single-particle level-spacing case would have a density proportional to U^2.

In both Ref. 1 and Ref. 2 some discrepancies between the data and the original formulation of the exciton model[3] were found. The authors of Ref. 2 suggest that the constant single-particle level-spacing assumption and pairing effects be investigated as possible causes for the observed inconsistencies.

In the present experiment, data for the $^{51}V(p,n)$-^{51}Cr reaction were obtained over a more extended range of bombarding energies to examine the extent to which the previous analyses were influenced by the relatively narrow range of bombarding energies for which data were available. An evaluation of the constant level-spacing assumption was made by calculating the particle-hole state densities using a Nilsson basis. The role of pairing shifts in modifying spectral shapes was also examined.

Finally, the experimental spectra were compared with the values calculated from the hybrid model, an exciton model in which the assumption of a constant matrix element for all two-body interactions is avoided by using information obtained from nucleon-nucleon scattering to estimate intermediate state lifetimes.

II. EXPERIMENTAL PROCEDURE

Protons with energies from 18 to 26 MeV were provided by the Lawrence Livermore Laboratory cyclograaff. This two-component machine consists of a 15-MeV AVF cyclotron and an EN tan-

dem Van de Graaff accelerator in series. An external sweeper served to eliminate four cyclotron pulses out of every five, reducing the frequency of the beam from 25 to 5 MHz before injection into the tandem. The resultant separation between bursts allowed the neutron spectrum to be measured without overlap from the end point down to about 5 MeV. A multidetector array located 10.8 m from the target allowed acquisition of data at 10 angles simultaneously. Figure 1 shows angle-integrated cross sections obtained at the five bombarding energies. Differential energy spectra were summed in 1-MeV bins for angles between 24 and 144°; these cross sections were fitted with a five-term Legendre expansion to obtain integrated cross sections. The integrals were insensitive to the order of the polynomials used in the fitting.

III. ANALYSIS AND RESULTS

The exciton model[3-6] for nonequilibrium reactions is based on the postulate that the compound nucleus reaches equilibrium through a series of two-body interactions. If at each stage a small width for particle decay is assumed in addition to the width for decay into more complicated states, a nonequilibrium component will be added to the emission spectrum. Under the assumption that the level densities for various particle-hole states can be calculated from a basis of equidistant single-particle levels (constant spacing assumption), and that the matrix elements for all transitions involving a two-body interaction are equal, the following expression[5] for the emission spectrum may be obtained:

$$\sigma(\epsilon) \propto \frac{\epsilon \sigma_{\text{inv}}}{(gE^*)^3} \sum_{\substack{n=n_0 \\ \Delta n=2}} (U/E^*)^{n-2}(n^3 - n), \tag{1}$$

where $\sigma(\epsilon)$ is the cross section for emission of a particle of energy ϵ, σ_{inv} is the inverse capture cross section, g is the density of single-particle states, E^* is the excitation energy in the composite system, and U is the excitation energy in the residual nucleus. The parameter n corresponds to the exciton number (where an exciton denotes either a particle or a hole) of the state from which decay occurs. n_0 corresponds to the first-formed intermediate state from which decay can occur and successive terms in the power series correspond to decay at later stages in the equilibration process. $\bar{n}$ denotes the exciton number beyond which the branching ratios will be given by the usual statistical calculations.

For the most energetic neutrons, U/E^* will be small and the leading term in the series will be expected to dominate. In this case, Eq. (1) may be rewritten

$$\sigma(\epsilon) \propto \epsilon \sigma_{\text{inv}} \rho_{n-1}(U), \tag{2}$$

where $\rho_{n-1}(U)$ is the density of $(n-1)$-exciton states at an energy U. If the state densities are calculated with a constant spacing model, $\rho_{n-1}(U)$ will be proportional to U^{n-2}. Thus, Eq. (2) becomes

$$\sigma(\epsilon) \propto \epsilon \sigma_{\text{inv}} U^{n-2}. \tag{3}$$

Griffin[3] has predicted that the values 3 and 4 for n_0 would be observed for even- and odd-A targets, respectively, with the result that the U dependence of Eq. (3) will be linear or quadratic, respectively. Thus, for the $^{51}V(p,n)$ reaction, a U^2 dependence would be consistent with Griffin's assumption.

A previous study[7] of the $^{51}V(p,n)^{51}Cr$ reaction at lower energies yielded results which were not completely consistent with this prediction. The

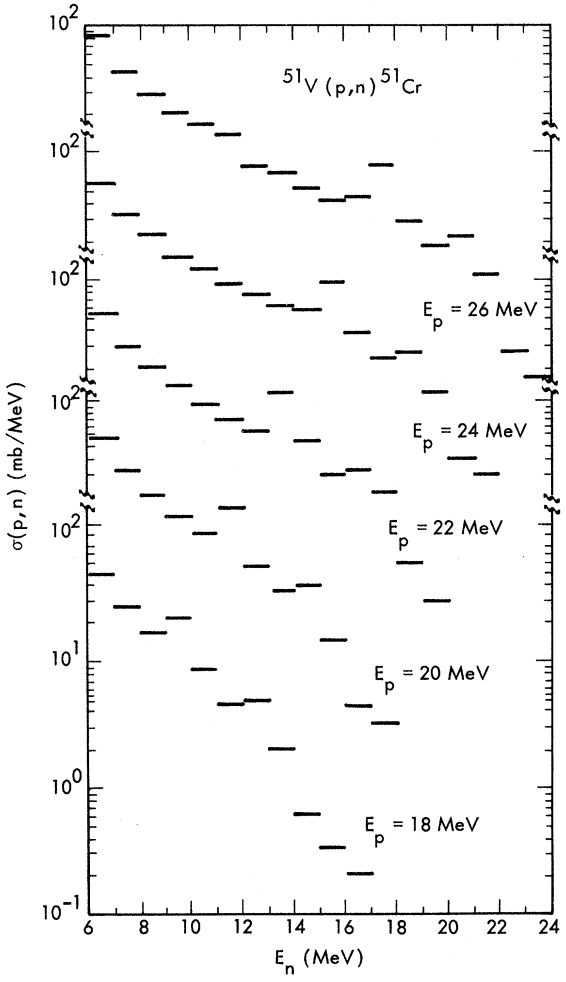

FIG. 1. Angle-integrated cross sections for the $^{51}V(p,n)^{51}Cr$ reaction at E_p = 18, 20, 22, 24, and 26 MeV.

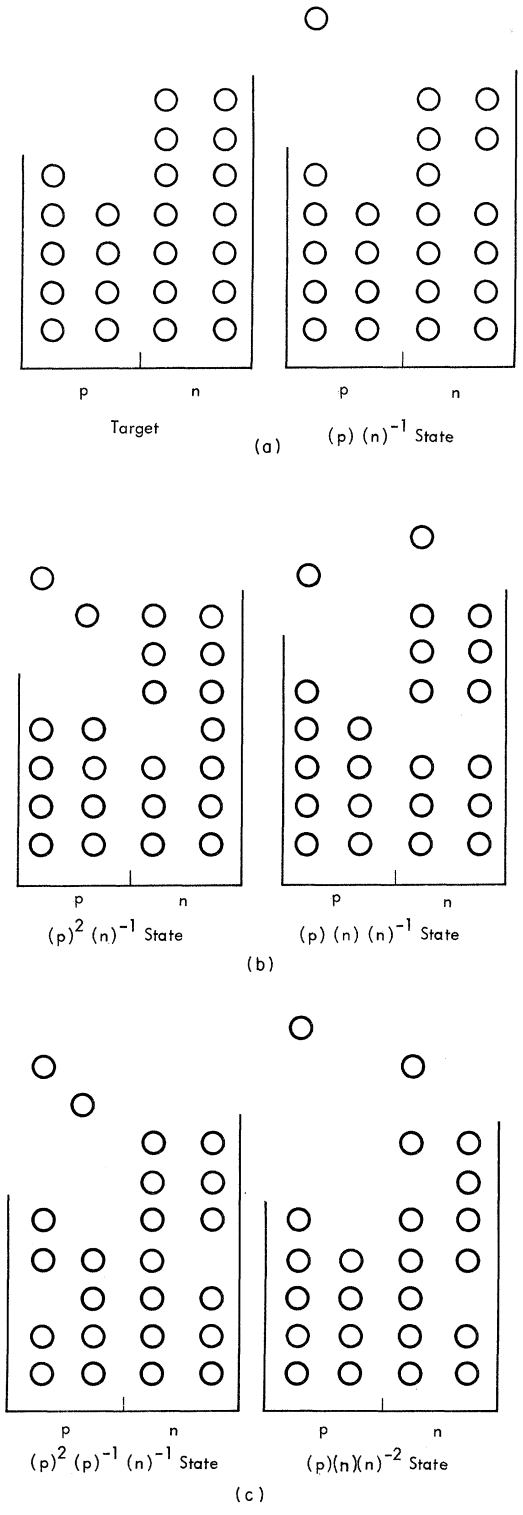

FIG. 2. Schematic representations of states of various exciton configurations: (a) Ground state of the target and a $(p)(n)^{-1}$ state; (b) $(p)^2(n)^{-1}$ and $(p)(n)(n)^{-1}$ states; (c) $(p)^2(p)^{-1}(n)^{-1}$ and $(p)(n)(n)^{-1}$ states.

bombarding energies at which the data of Ref. 7 were obtained were sufficiently low, however, that equilibrium contributions were not negligible even for low excitation energies in the residual nucleus. An attempt was made to subtract this component from the spectra, but the results were necessarily less definitive than would be obtained if the equilibrium component were unimportant in the energy region of interest. In addition, if the analysis is extended to energies as high as 9 MeV in the residual nucleus, the assumption that higher terms in Eq. (1) can be neglected would be easier to justify for higher bombarding energies (larger E^*).

As has been pointed out previously,[2] differences between n values for neighboring odd and even nuclei could arise from effects other than the participation of the unpaired nucleon in the reaction. For the nuclei studied in Ref. 2, both shell and pairing effects were found to produce differences in spectral shape between neighboring nuclei.

To investigate the role of these factors in determining the shape of the $^{51}V(p, n)$ spectra, the constant spacing assumption was abandoned and instead single-particle-state energies for protons and neutrons obtained from a Nilsson calculation[8] were used. These were folded together[9] to give the appropriate particle-hole-state densities. Such a calculation includes shell effects but not the effects of pairing. A correction for pairing was made by shifting the energy by the amount corresponding to the number of broken pairs relative to the ground state of ^{51}Cr. Because the number of broken pairs is small in the states of interest, the constant energy shift per broken pair should be a reasonably accurate approximation to a more exact calculation[10,11] of pairing effects. The magnitude of the shift was taken to be 1.8 MeV.

Schematic representation of the configurations of interest are shown in Figs. 2(a)–(c). If the re-

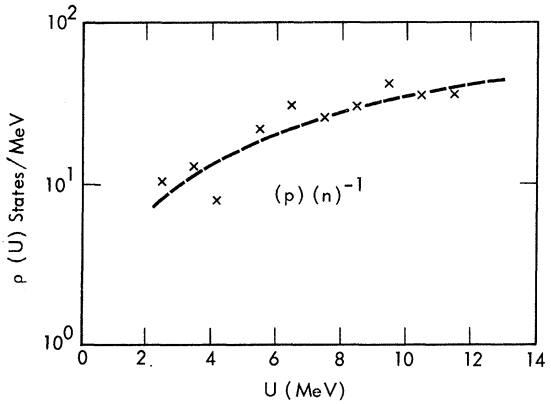

FIG. 3. Calculated state density for the configuration $(p)(n)^{-1}$. The dashed line is a fit of the form $\rho(U) \propto U$ to the calculated values.

action proceeds through a two-particle–one-hole state which decays to a one-particle–one-hole state, the final states will have the configuration one-proton–one-neutron-hole $[(p)(n)^{-1}]$ relative to the target ground state. For odd-A targets, Griffin assumes that the odd nucleon is also scattered in the reaction; in such a case, the final states are of two-proton–one-neutron-hole $[(p)^2(n)^{-1}]$ type, where the notation omits reference to the additional proton hole, because it is fixed and does not represent a degree of freedom. For an odd-A–odd-Z target, however, the residual nucleus reached in a (p, n) reaction is odd in N rather than Z; thus, it might be as plausible to assume excitation of the unpaired neutron in the final nucleus as the unpaired proton in the target. This configuration is denoted $(p)(n)(n)^{-1}$, where again the additional neutron hole is not included in the notation because it is fixed relative to the first hole and thus does not represent an additional degree of freedom.

The remaining two types of states shown in Fig. 2(c) are those characterized by an additional particle-hole pair relative to the $(p)(n)^{-1}$ states. If the spectra contain contributions from the decay of three-particle–two-hole states, residual states would be expected to be of $(p)^2(p)^{-1}(n)^{-1}$ or $(p)(n)(n)^{-2}$ type. Calculations with pairing shifts of the state density for these five configurations are shown in Figs. 3–5.

Also shown on these figures as dashed curves is the best fit of the form U^n $(0 \leq n \leq 6)$ to each calculated level density. The constant spacing model would predict the energy dependences U, U^2, U^2, U^3, and U^3 for configurations $(p)(n)^{-1}$,

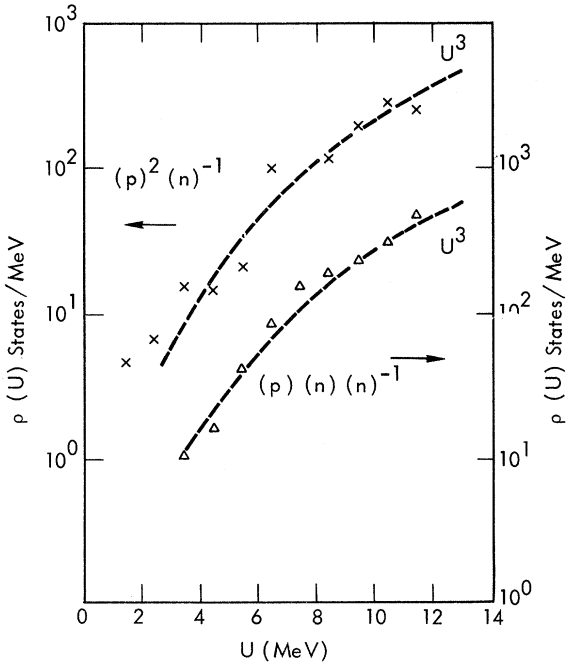

FIG. 4. Calculated state density for the configurations $(p)^2(n)^{-1}$ and $(p)(n)(n)^{-1}$. The dashed lines are fits of the form $\rho(U) \propto U^3$ to the data.

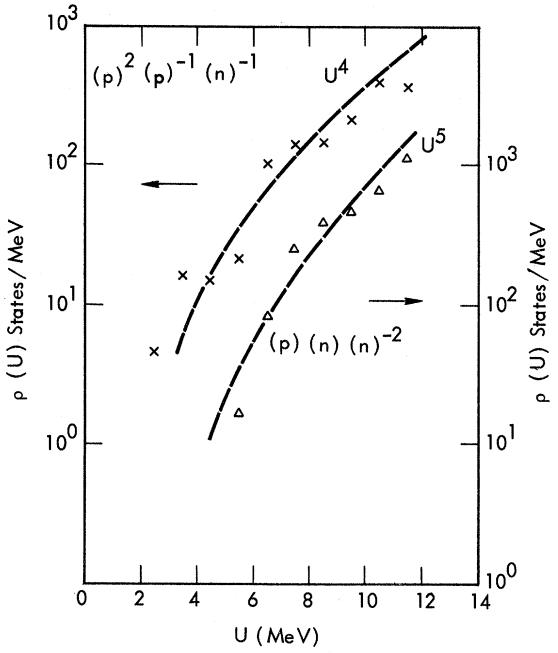

FIG. 5. Calculated state density for the configurations $(p)^2(p)^{-1}(n)^{-1}$ and $(p)(n)(n)^{-2}$. The dashed lines are fits of the forms $\rho(U) \propto U^4$ and $\rho(U) \propto U^5$, respectively, to the calculated values.

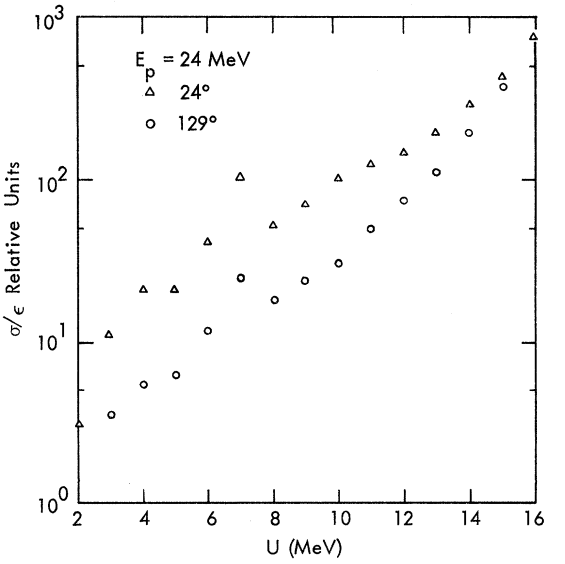

FIG. 6. Comparison of the spectra at 24 and 129° for E_p = 24 MeV.

$(p)(n)(n)^{-1}$, $(p)^2(n)^{-1}$, $(p)(n)(n)^{-2}$, and $(p)^2(p)^{-1}(n)^{-1}$, respectively. For all except the $(p)(n)^{-1}$ state density, the best-fit form was a higher power in U than predicted by the constant spacing model and, even in this case, the form U^2 gave almost as good a fit as the form U. Comparison of the calculations with and without pairing shifts established that the deviations from the constant spacing model predictions were due primarily to pairing effects. The conclusion that shell effects are not important in this mass region agrees with that of Ref. 12, but a similar study[2] of nuclei near the closed shell at Sn found significant shell effects in that mass region.

Because of the large volume of data and its smooth variation with angle and bombarding energy, only the angle-integrated data at each energy were compared with calculations. Figure 6 shows forward and backward-angle spectra at one energy, 24 MeV. The analog state (between 6 and 7 MeV in excitation energy) produces the only observable peak in the otherwise smooth energy dependence of the angle-integrated data. Three much smaller peaks at slightly lower excitation energy than the analog were observed in the forward-angle differential energy spectra. These are only barely observable in the same spectra averaged over 1-MeV intervals and therefore do not appear in the angle-integrated cross sections.

The spectra of Fig. 1 change significantly in shape between 18 and 26 MeV, such that at higher bombarding energies the cross section increases more slowly as a function of U. This behavior, as previously mentioned, may be a consequence of the fact that higher order terms in Eq. (1) cannot be ignored at the lower bombarding energies, because U is not sufficiently small relative to E^*. Comparison of the calculations with the data yielded the results shown in Figs. 7–11.

Fits to the experimental spectra were attempted with the calculated state densities shown in Figs. 3, 4, and 5. As would be expected from the changes in shape with bombarding energy, the forms corresponding to the best fit at low energies were not identical to those at higher energies.

The most unambiguous results were obtained at the three highest bombarding energies. For the 22-, 24-, and 26-MeV spectra (Figs. 7 and 8), the $(p)(n)^{-1}$ form clearly provided the best fit to the data. The importance of including pairing shifts was examined by fitting the unshifted $(p)(n)^{-1}$ level density to the data; a poorer fit resulted. Deviations from the calculated form are due to population of the analog state, which produces a

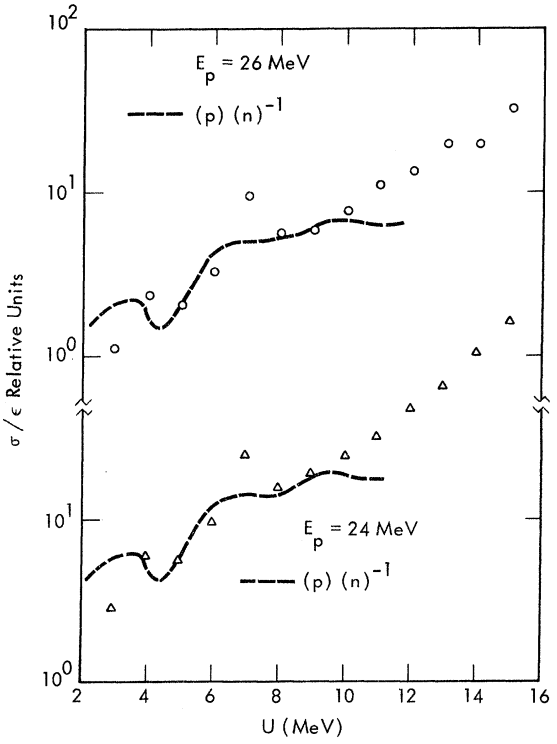

FIG. 7. Fits of the $(p)(n)^{-1}$ state density to the 24- and 26-MeV spectra.

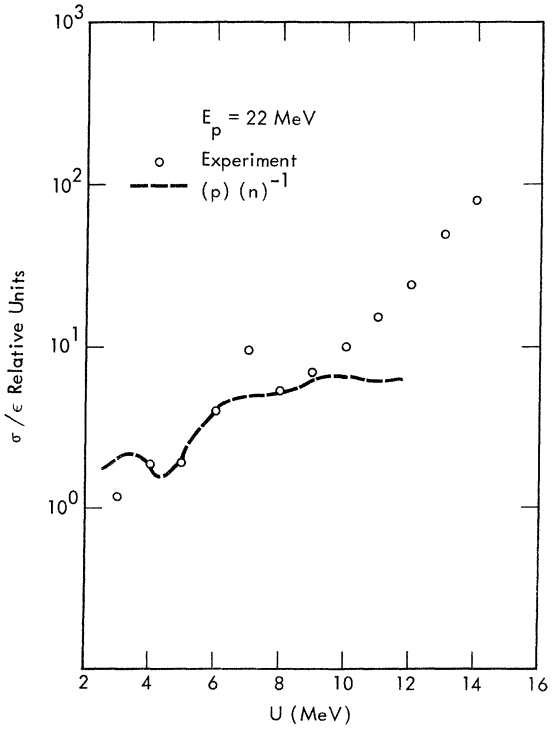

FIG. 8. Fit of the $(p)(n)^{-1}$ state density to the 22-MeV spectrum.

peak near 7-MeV excitation, and to contributions from equilibrium reactions and from higher terms in Eq. (1), which cause the data to be above the calculation for $U > 10$ MeV.

None of the calculated forms individually provided a good fit to the 18- or 20-MeV data, although the $(p)^2(n)^{-1}$ and $(p)(n)(n)^{-1}$ forms produced better agreement than the other three configurations. Figure 9 shows the fit of the $(p)^2(n)^{-1}$ form to the data at two energies; the fit is made to look better than it really is by the presence of the analog state where this form shows a steep rise. In fact, this peak should not be reproduced by the calculations.

Because no single form provided a good fit to the 18- and 20-MeV spectra, an effort was made to fit these data with a combination of two terms. According to the exciton model, the two terms which are likely to appear in addition to the $(p)(n)^{-1}$ state density are those corresponding to $(p)^2(p)^{-1}(n)^{-1}$ and $(p)(n)(n)^{-2}$ configurations, i.e., creation of an additional proton or neutron particle-hole state. The similar energy dependence of the state density for these latter two configurations makes it unnecessary to include both in the fits. The comparisons presented in Figs. 10 and 11 result from the use of the two terms corresponding to $(p)(n)^{-1}$ and $(p)^2(p)^{-1}(n)^{-1}$ configurations.

All of the spectra deviate from the two-term fit in the region of large U; these discrepancies are due to contributions from equilibrium pro-

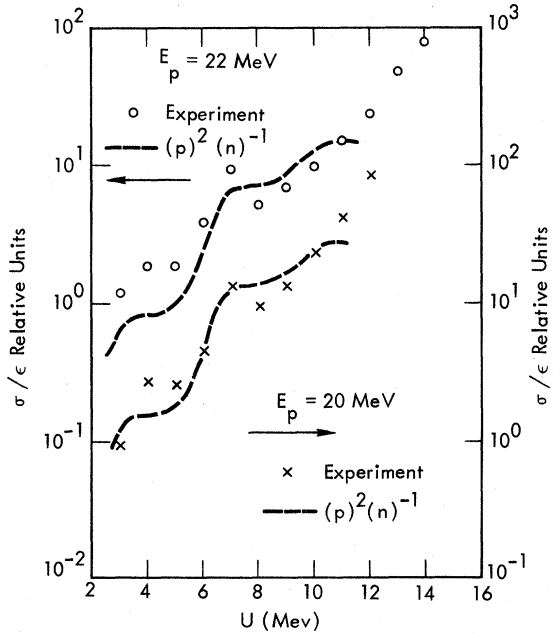

FIG. 9. Fits of the $(p)^2(n)^{-1}$ state density to the 20- and 22-MeV spectra.

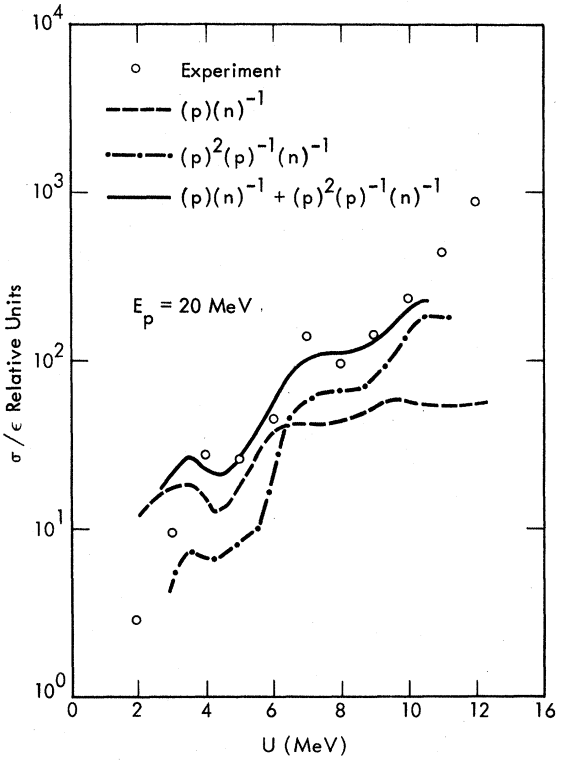

FIG. 10. Fit of a combination of the $(p)(n)^{-1}$ and $(p)^2(p)^{-1}(n)^{-1}$ state densities to the 20-MeV spectrum.

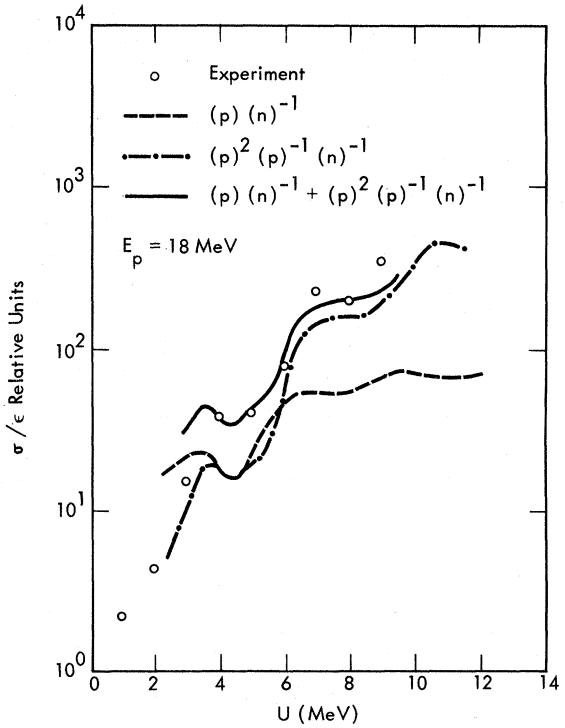

FIG. 11. Fit of a combination of the $(p)(n)^{-1}$ and $(p)^2(p)^{-1}(n)^{-1}$ state densities to the 18-MeV spectrum.

cesses. Based on the results at lower bombarding energies, these reactions are not expected to dominate the cross section in the region of low residual excitation, but a large portion of the neutron cross section corresponding to excitations 10 MeV and above would correspond to equilibrium processes. An attempt was made to fit the 18-MeV spectrum with the $(p)(n)^{-1}$ state density and contribution from equilibrium reactions with level density parameters obtained from Ref. 7; this resulted in poorer fits than were obtained with the two-term fit shown in Fig. 11 and provides support for the interpretation that deviations from the $(p)(n)^{-1}$ shape are not entirely due to contributions from equilibrium processes. A slight improvement in the quality of the fits could be obtained by increasing the pairing shift slightly; this was not done because it was felt that the agreement was within the limits of significance of the calculation because of the neglect of residual interactions other than pairing.

A final comparison between the exciton model and the data was made by examining the bombarding energy dependence of the (p, n) cross section at a given excitation energy U. Assuming $n_0 = 3$ and using the fact that for small U the first term of Eq. (1) should dominate, the cross section $\sigma(\epsilon)$ divided by the energy ϵ should decrease as $(E^*)^{-4}$ with increasing excitation in the compound system. The fraction of the cross section corresponding to decay of the first stage preequilibrium states was estimated from the fits shown in Figs. 7, 8, 10, and 11; Fig. 12 presents the excitation energy dependence of this cross section. The observed dependence on E^* is $(E^*)^{-5}$, which is close to the predicted value. A slightly more rapid falloff could reflect some energy dependence in the matrix element coupling n-exciton states to $(n+2)$-exciton states. This interaction was assumed to be independent of energy in the derivation of Eq. (1). Alternatively, the density of n-exciton states at high energies in the compound system may not be given with sufficient accuracy by the form (U^{n-1}) obtained under the assumption that the single-particle levels are equidistant. In general, it would be expected that the single-particle density would increase with increasing energy, which would cause the n-exciton level densities to increase more rapidly than predicted by the constant spacing model. This deviation is in the proper direction to explain the observed more rapid energy dependence.

IV. HYBRID-MODEL CALCULATIONS

The exciton model as originally formulated does not predict absolute cross sections. As was discussed in Sec. III, it is normally assumed that matrix elements for all transitions involving a two-body interaction are equal; this assumption is needed to give the relative magnitude of various terms in the sum of Eq. (1). Because the strength of this interaction determines the branching ratio between continuum decay and damping into more complicated states, a value for this matrix element must be assumed in order to obtain an absolute value for the preequilibrium emission cross section.

Blann[13] has suggested that the constant matrix element assumption be abandoned and that the lifetime of the intermediate states of interest be determined through use of nucleon-nucleon cross sections. This model, called the hybrid model, has since been extended[14] to include the effects of the variation in nuclear density with radius and the limitation in the number of hole states caused by the finite depth of the potential. More recently, values of the optical-model imaginary potential have been used to deduce intermediate state lifetimes. For this model, the probability $p_x(\epsilon)d\epsilon$ of emission of a particle of type x in the

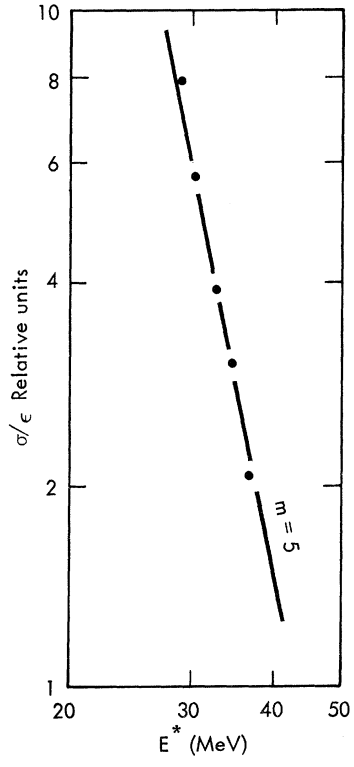

FIG. 12. Dependence on energy in the compound system (E*) of the $^{51}V(p,n)$ cross section for neutrons leaving the residual nucleus with excitation energy between 3 and 4 MeV. The solid line indicates the best fit of the form $(E^*)^{-m}$ to the data.

channel energy range ϵ to $\epsilon + d\epsilon$ is given by

$$p_x(\epsilon)d\epsilon = \sum_{\substack{n=n_0 \\ \Delta n=2}}^{\bar{n}} \left[{}_n p_x \frac{\rho_n(U,\epsilon)}{\rho_n(E^*)} g d\epsilon \right] \left[\frac{\lambda_c(\epsilon)}{\lambda_c(\epsilon)+\lambda_+(\epsilon)} \right] D_n \,. \tag{4}$$

In this expression, ${}_n p_x$ is the number of particles of type x in an n-exciton state, $\rho_n(E^*)$ is the density of n-exciton states at an energy E^*, $\rho_n(U,\epsilon)$ is the density of n-exciton states such that $n-1$ excitons share an energy U and the remaining exciton has an energy equal to its binding energy B_x plus ϵ, and g is the density of single-particle states per MeV. $\lambda_c(\epsilon)$ and $\lambda_+(\epsilon)$ are the rates at which particles of energy $B_x+\epsilon$ are emitted into the continuum or scattered with the formation of an additional particle-hole state, respectively. D_n is a depletion factor, which gives the relative flux reaching an n-exciton state before decay occurs. The continuum decay rate $\lambda_c(\epsilon)$ is given by

$$\lambda_c(\epsilon) = \sigma_v v \rho_c / gV \,, \tag{5}$$

where σ_v is the inverse cross section and v the velocity of a particle having ρ_c states in the continuum. The parameter V is an arbitrary volume and cancels the same volume in ρ_c. Blann includes geometry-dependent effects by making the parameter $\lambda_+(\epsilon)$ a function of l, which is plausible physically because of the dependence of the former quantity on nuclear density, and hence impact parameter.

The resulting cross section is then

$$\frac{d\sigma_x(\epsilon)}{d\epsilon} = \pi \lambda^2 \sum_{l=0} (2l+1) T_l p_x(\epsilon) \,, \tag{6}$$

where T_l is the transmission coefficient for orbital angular momentum l in the entrance channel and $p_x(\epsilon)$ is given by Eq. (4); the l dependence of this latter quantity enters implicitly through the dependence of $\lambda_+(\epsilon)$ on l.

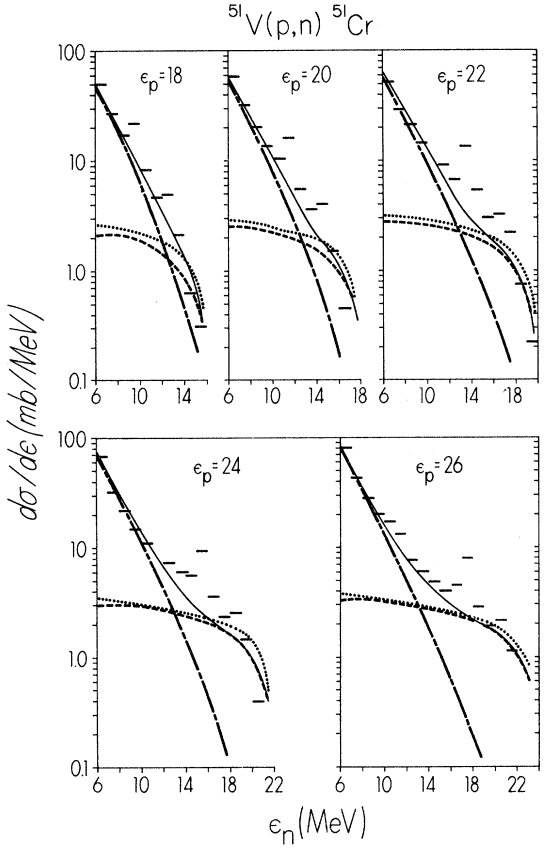

FIG. 13. Comparison of measured neutron spectra with those calculated from the hybrid model. The dotted and dashed curves are the preequilibrium components calculated with intermediate state lifetimes calculated from the optical-model and nucleon-nucleon cross sections, respectively. The dot-dashed curve represents the neutron spectrum from equilibrium reactions and the solid curve is the sum of the equilibrium and preequilibrium (dashed) contributions.

Calculations of the preequilibrium spectrum using Eq. (4) are presented in Fig. 13. The dotted curve is the preequilibrium spectrum obtained with $\lambda_+(\epsilon)$ values determined from the optical-model imaginary potential of Becchetti and Greenlees[15]; the dashed curve of similar shape is the corresponding calculation for $\lambda_+(\epsilon)$ values[14] determined from nucleon-nucleon scattering cross sections. The steeper dot-dashed curve represents the neutron spectrum from equilibrium reactions and the solid curve is the sum of the equilibrium and preequilibrium (dashed) contributions. Considering the uncertainties in such a calculation, the agreement in both shape and magnitude is quite impressive. The dependence of the cross section on both excitation and bombarding energy is well described by the calculations. The good agreement between experiment and calculations using either nucleon-nucleon cross sections or the optical-model imaginary potential to deduce lifetimes of intermediate states suggests that either procedure yields reasonable results.

V. SUMMARY

Comparison of neutron spectra produced in the $^{51}V(p,n)^{51}Cr$ reaction with shapes calculated from the exciton model yields good agreement under the assumption that the first-formed intermediate state is of two-particle–one-hole character. For the data at 22, 24, and 26 MeV, the contribution from decays to one-particle–one-hole states dominates the spectrum for residual excitations less than 10 MeV. At lower bombarding energies, the next higher term, corresponding to two-parti-

cle–two-hole states in the residual nucleus must also be included to fit the data in this energy range.

The measured spectra were also compared to cross sections calculated with the hybrid model. Good agreement in both shape and magnitude was observed. Use of nucleon-nucleon cross sections to determine the intermediate state lifetime produced results very similar to those obtained with lifetimes determined from the optical model.

ACKNOWLEDGMENT

The authors would like to thank Professor M. Blann for performing the calculations presented in Sec. IV.

---

*Work performed under the auspices of the U.S. Atomic Energy Commission.

[1]E. V. Lee and J. J. Griffin, Phys. Rev. C 5, 1713 (1972).
[2]S. M. Grimes, J. D. Anderson, J. W. McClure, B. A. Pohl, and C. Wong, Phys. Rev. C 7, 343 (1973).
[3]J. J. Griffin, Phys. Rev. Lett. 17, 478 (1966).
[4]M. Blann, Phys. Rev. Lett. 21, 1357 (1968).
[5]F. C. Williams, Jr., Phys. Lett. 31B, 184 (1970).
[6]C. K. Cline and M. Blann, Nucl. Phys. A172, 225 (1971).
[7]S. M. Grimes, J. D. Anderson, J. W. McClure, B. A. Pohl, and C. Wong, Phys. Rev. C 3, 645 (1971).
[8]S. G. Nilsson, K. Dan. Vidensk. Selsk. Mat.-Fys. Medd. 29, No. 16 (1955).
[9]A computer code (written by F. C. Williams, Jr.) for such calculations was supplied to the authors by Professor M. Blann of the University of Rochester.
[10]A. Bohr, B. Mottelson, and D. Pines, Phys. Rev. 110, 936 (1958).
[11]A. M. Lane, *Nuclear Theory* (Benjamin, New York, 1964), p. 19.
[12]S. M. Grimes, J. D. Anderson, J. W. McClure, B. A. Pohl, and C. Wong, Phys. Rev. C 5, 830 (1972).
[13]M. Blann, Phys. Rev. Lett. 27, 337 (1971).
[14]M. Blann, Phys. Rev. Lett. 28, 757 (1972); to be published.
[15]F. D. Becchetti and G. W. Greenlees, Phys. Rev. 182, 1190 (1969).